

Fast Optic Disc Segmentation in Retinal Images Using Polar Transform

Muhammad Nauman Zahoor and Muhammad Moazam Fraz^(✉)

School of Electrical Engineering and Computer Science,
National University of Sciences and Technology, Islamabad, Pakistan
{14mscsmzahoor, moazam.fraz}@seecs.edu.pk

Abstract. Glaucoma is one among major causes of blindness. Early detection of glaucoma through automated retinal image analysis helps in preventing vision loss. Optic Disc segmentation from retinal images is considered as the preliminary step in developing the diagnostic tool for early Glaucoma detection. A novel hierarchical technique for optic disc localization and segmentation on retinal fundus images is presented in this paper. Retinal vasculature and pathologies are delineate and removed by using morphological operations as preprocessing steps. Circular Hough transform is used to localize the optic disc. Region of interest is calculated and a novel polar transform based adaptive thresholding is performed to obtain the precise boundary of optic disc. The methodology has shown considerable improvement over existing methods in terms of accuracy and processing time. The algorithm is evaluated on a number of publicly available retinal image sets which includes MESSIDOR, DIA-RETDB1, DRIONS-DB, HRF, DRIVE and RIM-ONE, with average spatial overlap approximately 85%.

Keywords: Optic disc · Retinal image analysis · Polar transform · Segmentation · Glaucoma

1 Introduction

The automated analysis of human retinal images has been widely used for early detection, screening and treatment planning of various retinal, ophthalmic and systemic disease. Retinal image analysis had been increasingly used in large scale screening programs and population based studies for early detection of glaucoma and diabetic retinopathy [1]. The analysis of change in morphological attributes of retinal anatomical structures including Optic Disc (OD), Optic Cup, retinal vasculature and pathologies triggers timely detection and treatment of glaucoma while it is still in early stage [2]. Early detection and hence treatment can help in prognosis of vision loss. The precise segmentation of OD is the preliminary step in development of computer assisted automated system for glaucoma screening. OD is distinguished as a variable sized slightly yellowish elliptical area in the retinal images. The ganglion cell axons leave the eye, forming an optic nerve which transmits the visual information to the brain. The OD has two prominent regions; central brighter region and the peripheral region containing OD cup which is also termed as the neuro-retinal rim [1]. The Optic Disc and other anatomical features in retinal image is shown in Fig. 1.

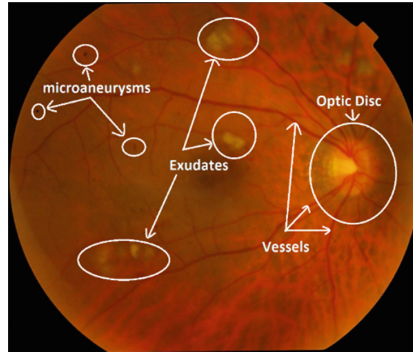


Fig. 1. Retinal features on fundus image

Glaucoma is characterized by the change in color, shape and depth of OD. The presence of parapapillary atrophy produces bright regions around the OD rim distorting the elliptical shape [1]. Moreover, the progression in optic nerve fiber damage causes the structural changes in OD, optic nerve head and nerve fiber layer which results in an increase in optic cup to disc ratio (CDR). The CDR can be accessed by estimating the diameter and the area of OD, the area of rim and optic cup diameter. The accurate and fast OD segmentation and analysis is the first step towards the development of computer assisted diagnostic system for glaucoma screening in large population based studies.

Retinal pathologies which includes exudates, hemorrhages and other bright lesions, if present, may look similar in appearance to the shape of OD, thus may result in false detection. Hence the robust localization and segmentation of OD is a challenging task because of various factors like presence of pathologies and other anatomical structures, uneven illumination, variability in luminosity and contrast during image acquisition. Moreover, the presence of incoming blood vessels make the OD boundary appeared as non-distinctive fused boundary.

This paper presents a new hybrid approach for fast and accurate localization and segmentation of OD based on Circular Hough Transform (CHT) [3] and Polar Transformation algorithm [4]. The Polar Transformation algorithm has been widely used in many application areas of image segmentation, but has not been applied within the framework of retinal image analysis. To the limit of our knowledge, the Polar Transform (PT) algorithm has been utilized for the first time in localizing and segmenting OD in retinal images. Experimental evaluation shows that this method is computationally fast in processing, robust to the variation in image contrast and illumination, and comparable with the state of the art methodologies in terms of quantitative performance metrics.

It's worth mentioning that the proposed methodology is aimed at contributing to the development of computer assisted system for glaucoma screening. There are other published methods of OD segmentation available in literature but this methodology is computationally fast, produces higher accuracy, robustness and tolerant to vast variety of images as shown by the use of various retinal fundus datasets made up of diseased and healthy images. This all make it suitable for integration with glaucoma detection system.

The organization of the paper is as follows. A comprehensive review OD detection and segmentation methodologies is presented in Sect. 2. The proposed methodology is explained in Sect. 3. The materials and the performance metrics used to evaluate the proposed methodology are illustrated in Sect. 4. The evaluation results and comparative analysis with other methods is presented in Sect. 5. Section 6 concludes the paper.

2 Related Work

There are a number of methodologies available in literature for Optic Disc Segmentation. Some preliminary work involves the segmentation by modeling the OD as an elliptical or a circular object [5] and performing the shape-based template matching. The irregularity in the shape of OD, the presence of the pathological structures and the difference in the multiple views of OD are the challenges faced by the shape based modeling methodologies. Active contour models had been utilized for OD segmentation. Contours were initialized manually as well as automatically and the energy term; derived from the gradient of image, caused the deformation of the contour. The OD boundary was detected by employing the gradient vector flow based active contour model [6]. The energy minimization was achieved by the using pre-processed images or by applying the constraint on the OD segmentation results to elliptical or circular region [7]. The snake model [8] has also been proposed to improve the OD segmentation in the presence of vessel occlusion. Watershed transformation has also been used to detect the OD contour [9]. Geometric active contour model in combination with maximum local variance has been proposed by Kande et al. [10]. Optic Disc was detected by Staporet et al. [11] using geodesic reconstruction by dilation and extracted Optic Disc using Mathematical Morphology. Lupascu et al. [12] approximated Optic Disc boundary by using texture information and applying a regression based technique to obtain the best circle that defines the OD boundary. Detection and Extraction of Optic Disc was done without assuming any pre-defined shape using mathematical morphology techniques by Welfer et al. [13]. Basit and Fraz [14] used marker controlled watershed transform for Optic Disc segmentation. After application of morphological operations and smoothing filters, gradient magnitude image was modified using Internal and external markers and watershed transformation was applied for OD boundary extraction. A combination of morphological template based technique followed by CHT, was used by Aquino et al. [15]. Principal Component Analysis based mathematical modelling was proposed by Morales et al. [16]. Abdullah et al. [17] had used morphological operation and grow cut algorithm for approximating the OD boundary.

3 Proposed Methodology

This work presents an automated Optic Disc localization and segmentation technique that is able to detect OD without using any initial vascular information and template knowledge. For the segmentation of OD boundary, the first step is to approximate the OD center. Optic Disc appears as the brightest spot in the retinal fundus images but the

presence of artifacts can create multiple bright spots. Pathologies in fundus images can take shape of OD while actual OD could lose its brightness. As shown in Fig. 3. The shape of the OD varies from circular to elliptical. This information about the shape of the OD can be used for the detection of OD. The proposed methodology preprocesses the image to remove vessels and enhance the OD boundary using morphological operations. CHT is used for OD localization. Spatial to polar transform is applied to convert circular region of interest into rectangular. Adaptive thresholding is applied to obtain the OD boundary. Flow chart of the proposed methodology is presented in Fig. 2.

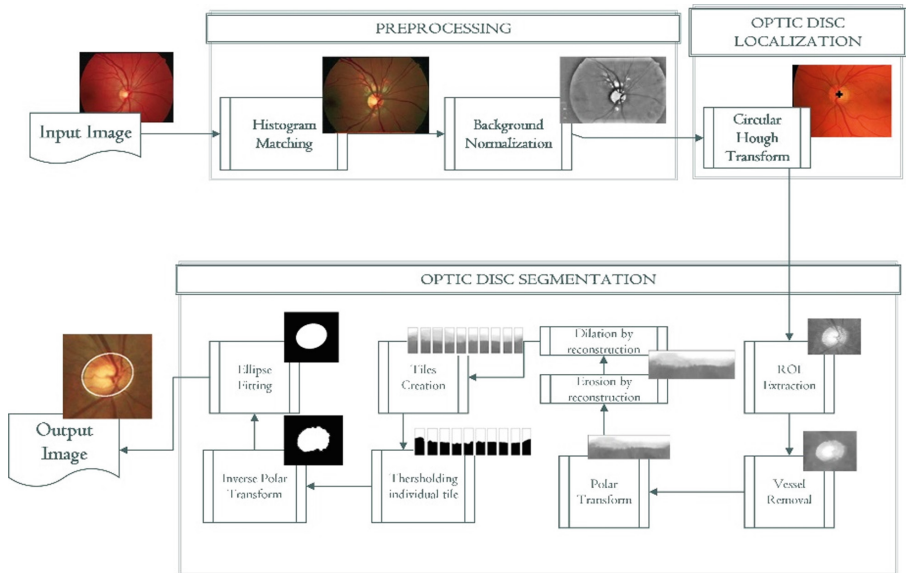


Fig. 2. Proposed methodology workflow

3.1 Preprocessing

Varying conditions during image capture, noise, and uneven illumination and contrast variations are the added challenges of automated optic disc detection and segmentation. Figure 3 shows retinal images under different illumination conditions and affected with pathologies. In order to handle these images autonomously, preprocessing has to be applied.

Histogram Matching [18] has been applied for normalizing the image variations. The histogram of properly illuminated image (Fig. 4(a)) is taken as reference and the other images' histograms are matched with it which resulted in normalized illumination and color tone. Red channel was chosen as it contains most information of the Optic Disc. Background normalization is then performed by subtracting the image with the estimate of background. The estimate of background I_{bg} is calculated by filtering the image with a large arithmetic mean kernel such that the filtered image doesn't contain

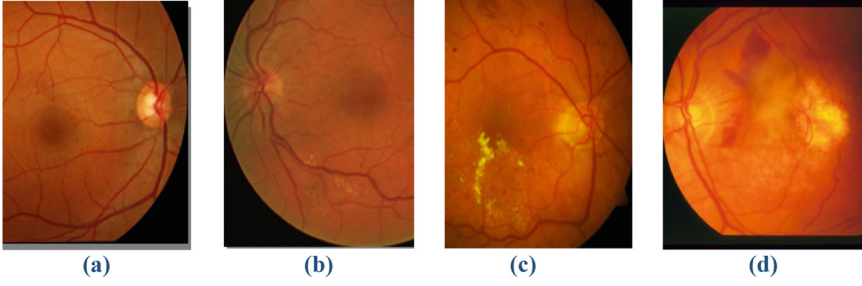


Fig. 3. Different modalities of optic disc (a) OD is bright and visible. (b) OD is not bright. (c) OD is bright together with pathologies. (d) OD with pathologies.

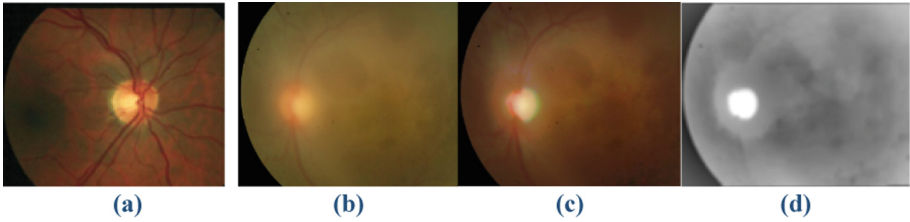


Fig. 4. Preprocessing. (a) Reference image to be matched with. (b) Images under different illumination and reflectance. (c) Image after histogram matching. (d) Red channel background normalized image. (Color figure online)

any visible structures. Original image is also morphologically opened using a ‘disk’ shaped structuring element with a size $1/100th$ the size of the original image to obtain I_{open} . The size $1/100th$ of actual image was chosen after manual experimentation on various image databases and keeping the overall best performing size. Background normalized image $I_{normalized}$ is the difference of opened image and the background estimate, as shown in Eq. (1).

$$I_{normalized} = I_{open} - I_{bg} \quad (1)$$

Figure 4 shows the results of histogram matching and background normalization.

3.2 Optic Disc Localization

OD localization from preprocessed images is done by applying CHT which is an extension of Hough transform [19] which detects circular objects in the image. This step requires a radius search range of min radius and a max radius. Max and min radius are approximated to be $1/30th$ to $1/10th$ of the image width. This radius range covers the Optic Discs in the various image databases and disregards the effects of pathologies in the images. The output of the transform contains all the circles that are present in the given range. The circle with the highest score is kept. Figure 5 shows detected OD.

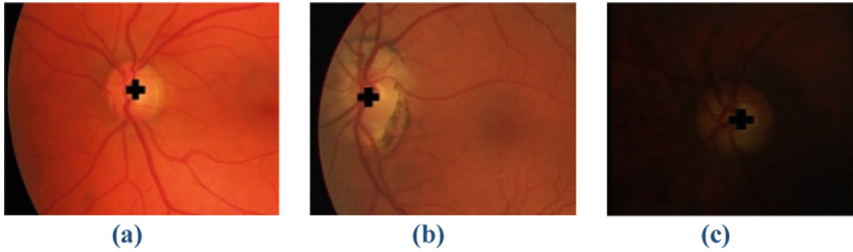


Fig. 5. Optic disc detection results via circular hough transform on normal and pathological images under challenging illumination settings

From the results it is clear that the OD localization technique along with preprocessing methodology is robust and is even able to localize OD under challenging illumination conditions and in the presence of pathologies.

3.3 Optic Disc Segmentation

For the precise segmentation of the optic disc, a region of interest (ROI) is extracted from the original image “ I_{orig} ”. The size of “ I_{roi} ” from “ I_{orig} ” is calculated as described by following equation.

$$roi_{size} = r + buff \quad (2)$$

Where, r is the radius of the circle approximated by the CHT and “ $buff$ ” is the number of extra pixels that are not part of the OD but surrounds it. ROI is centered on the circle center approximated by the CHT. ROI contains optic disc pixels surrounded by non-od pixels. The next task is to find precise boundary between OD pixels and non OD pixels. Direct thresholding techniques does not yield good results as the gray level distribution of the OD and non-OD regions is not uniform and applying a global threshold fails. Applying a local threshold on a neighborhood of pixels also does not return good results because of the circular nature of the OD. To overcome these issues, a novel OD segmentation technique is proposed that makes use of Polar Transform (PT) [18].

Polar transform can be defined as a 2D coordinate system where every point is calculated using distance from a reference point and an angle from a reference direction. Polar transform has been used a lot in automated segmentation of iris from image as is done by [20]. To the limit of our knowledge, the PT algorithm has been utilized for the first time in localizing and segmenting OD in retinal images.

For OD segmentation, the ROI image is calculated and ROI’s pixel coordinates are converted from Cartesian to polar coordinates by applying Polar Transform with the origin point being the center of the ROI image. Due to this transformation, the OD is now straightened. Next this straightened OD is divide in to 10 equal sized sub-tiles. Morphological erosion by reconstruction [18] is applied on each tile followed by morphological dilation by reconstruction. At this step, since precise boundary of the

optic disc is needed, morphological opening and closing is avoided as this would also remove the structures in the retina that are to be used as the end boundary points to distinguish between optic disc pixels and the rest of the image. Opening by reconstruction preserves the shape of the components.

After application of opening by reconstruction, each tile is then thresholded using adaptive thresholding. If the output tile is successfully thresholded in to two regions, it is forwarded to the next step as is. If not, then a blank tile (all black) is forwarded. The tiles are then combined and Polar to Cartesian transformation is applied. Ellipse fitting is then performed using ellipse equation in which the boundary obtained via thresholding is used to draw an ellipse over it. This gives the precise OD boundary. All steps of OD segmentation are graphically illustrated in Fig. 6.

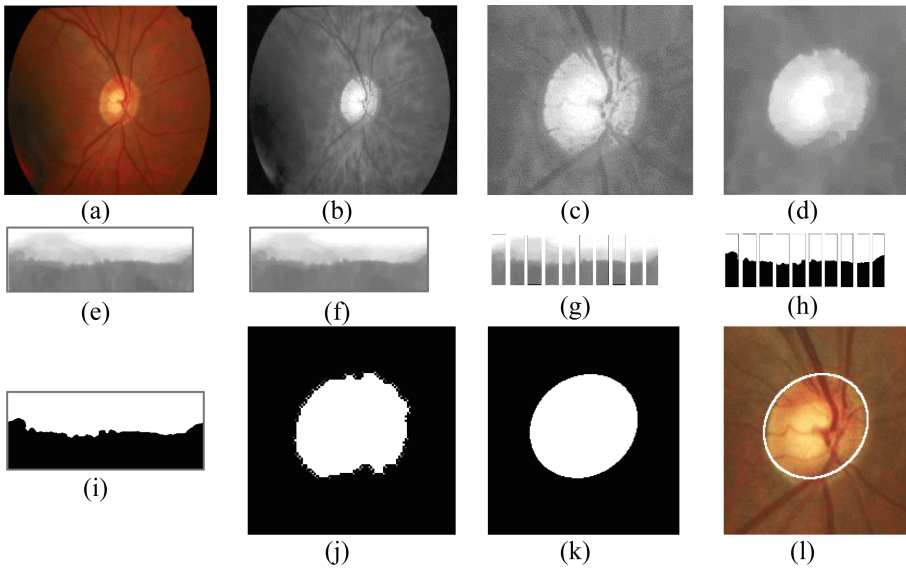


Fig. 6. Optic disc segmentation (a) Original image. (b) Red channel. (c) Region of interest ROI. (d) Vessels removed. (e) Cartesian to polar transform applied on ROI. (f) Morphological operations (erosion by reconstruction followed by dilation by reconstruction). (g) Segregation into tiles (h) Threshold application on individual tiles. (i) Thresholded tiles (j) Conversion from polar to cartesian. (k) Ellipse fitting. (l) Result overlay on the image.

4 Materials

The methodology is evaluated on following publically available datasets shown in Table 1 and a dataset received from a local hospital (Shifa international hospital).

Ground truths of OD boundary are available with RIM-ONE, HRF and Messidor databases whereas the images of DIARETDB1, DRIVE and DRIONS-DB were hand labeled by ophthalmic experts from the Armed forces institute of Ophthalmology, Rawalpindi by [17].

Table 1. Retinal image databases with count of images as healthy/pathological

	Database	Total images	Healthy	Diabetic retinopathy	Glaucomatous
1	RIM-ONE [21]	118	78	–	40
2	HRF [22]	45	15	14	15
3	MESSIDOR [23]	1200	540	660	–
4	DIARETDB1 [24]	89	05	84	–
5	DRIONS-DB [25]	110	06	83*	21
6	DRIVE [26]	40	33	07	–
7	Shifa database [17]	111	19	92	–

* Images with hypertensive retinopathy

Performance Measures

Pixel based comparison of ground truths and the OD segmentation obtained by the proposed methodology is presented. The four possible outcomes of pixel classification are illustrated in Table 2. Based on these outcomes, the calculated performance metrics are shown in Table 3.

Table 2. Classification of OD pixels

	Algorithm predicted pixel \in OD	Algorithm predicted pixel \notin OD
Actual pixel \in OD	True Positive (TP)	False Positive (FP)
Actual pixel \notin OD	False Negative (FN)	True Negative (TN)

Table 3. OD segmentation performance metrics

Measure	Description
SN	$TP/(TP + FN)$
SP	$TN/(TN + FP)$
Accuracy	$(TP + TN)/(TP + FP + TN + FN)$
Precision	$TP/(TP + FP)$
F1 Score	$2TP/(2TP + FP + FN)$
Overlap	$(\text{Predicted OD} \cap \text{Ground Truth OD})/(\text{Predicted OD} \cup \text{Ground Truth OD})$

5 Results

The optic disc segmentation results are shown in Fig. 7, where the OD boundary detected by the proposed methodology is shown in white marking. The quantitative performance metrics based on pixel-wise comparison of ground truths and the segmentation results obtained from the algorithm are shown in Table 4. The comparison with other methods are shown in Table 5. It is worth mentioning that the proposed methodology outperforms other techniques and uses less average time per image. The average time per image reported in Table 5 has been taken from the respective



Fig. 7. Results of OD segmentation on various dataset, contain images with uneven illumination conditions and affected with pathologies.

Table 4. OD segmentation quantitative performance measures

Database	Accuracy	Sensitivity	Specificity	Precision	F1 Score	Overlap
DRIONS-DB	0.9986	0.9384	0.9994	0.9463	0.9378	0.8862
DIARETDB1	0.9937	0.9706	0.9949	0.8991	0.9306	0.8734
HRF	0.9774	0.9233	0.9892	0.9448	0.9282	0.8686
SHIFA	0.9963	0.8908	0.9996	0.9873	0.9332	0.8788
MESSIDOR	0.9918	0.8891	0.9973	0.9537	0.9039	0.8441
RIM-ONE	0.9750	0.9112	0.9807	0.8310	0.8491	0.7480
DRIVE	0.9980	0.8309	0.9993	0.9136	0.8500	0.7561

Table 5. OD segmentation comparison with other techniques

DIARETDB1	Overlap	Sensitivity	Specificity	Accuracy	Time (in seconds)
Sopharak et al. [27]	0.294	0.4603	0.9994		
Kande et al. [10]	0.334	0.8808	0.9878		120.5
Seo et al. [28]	0.353	0.6103	0.9987		15.63
Walter et al. [29]	0.369	0.6569	0.9993		308.5
Lupascu et al. [12]	0.309	0.6848	0.9969		
Stapor et al. [11]	0.340	0.8498	0.9964		59.72
Basit and Fraz [14]	0.546	0.7347	0.9944		
Welfer et al. [13]	0.391	0.6341	0.9983		57.16
Abdullah et al. [17]	0.851	0.851	0.9984	0.9772	40
Proposed methodology	0.874	0.9706	0.9949	0.9937	1.3
DRIONS-DB					
Morales et al. [16]				0.9934	
Abdullah et al. [17]	0.851	0.8508	0.9966	0.9989	43.2
Proposed methodology	0.886	0.9384	0.9994	0.9986	1.6
MESSIDOR					
Morales et al. [16]				0.9949	
Abdullah et al. [17]	0.879	0.8954	0.9995	0.9989	71.3

(continued)

Table 5. (continued)

DIARETDB1	Overlap	Sensitivity	Specificity	Accuracy	Time (in seconds)
Proposed methodology	0.844	0.8891	0.9973	0.9918	1.8
DRIVE					
Sopharak et al. [27]	0.168	0.2104	0.9993		14.92
Kande et al. [10]	0.296	0.6999	0.9888		111.7
Seo et al. [28]	0.310	0.5029	0.9983		7.23
Walter et al. [29]	0.293	0.4988	0.9981		219.6
Salazar-Gonzalez et al. [30]		0.7512	0.9684	0.9412	
Lupascu et al. [12]	0.309	0.7768	0.9968		
Stapor et al. [11]	0.334	0.7368	0.9920		43
Basit and Fraz [14]	0.618	0.8921	0.9921		
Welfer et al. [13]	0.394	0.7357	0.9982		53.65
Abdullah et al. [17]	0.786	0.8188	0.9966	0.9672	59.2
Proposed methodology	0.756	0.8309	0.9993	0.9980	1.6

publications. We understand that hardware configuration should be taken into account for time comparison benchmarking with other methodologies, which we will do in the future.

6 Discussion and conclusion

Fast and precise segmentation of OD in varying imaging conditions is the preliminary step in development of automated system for glaucoma detection. The correct and precise segmentation of the optic disc will increase the correct diagnosis. A novel optic detection and segmentation methodology has been presented in this paper. The methodology has used hierarchical combination of morphological operations and CHT for the Optic Disc localization. This gives better results as relying only on the ‘‘Optic Disc as the brightest spot’’ technique that is used a lot for the detection purposes can give false results in presence of pathologies and poor illumination setting of optic disc. After detection, a novel polar transform based adaptive thresholding is applied. Based on OD localization, the circular ROI is extracted followed by the application of Polar transform for converting the ROI into distinct rectangular tiles. The tiles are adaptively thresholded to get the precise OD boundary. Inverse polar transform is then applied to get the OD shape back. To the best of our knowledge, the polar transformation has been applied for the first time for the segmentation of Optic Disc.

Evaluation was performed on publically available datasets that are MESSIDOR, DRIVE, HRF, DIARETDB1, RIM-ONE, DRIONS-DB and a dataset received from a local hospital. The outcome shows that the methodology is computationally efficient

and performs well even in varying illumination setting and contrast changes and in the presence of pathologies in the image. Optic Disc Segmentation Algorithm was able to achieve an average spatial overlap of 84.4% for MESSIDOR, 87.3% for DIRETDB1, 88.6% for DRIONS-DB, 86.9% for HRF, 75.6% for Drive and 74.8% for RIM-ONE. It has been observed that the proposed methodology segments the OD in images affected with pathologies and under varying illumination in less amount of time without compromising on accuracy.

We have already developed an automated software titled QUARTZ [2], for extraction of quantifiable parameters from retinal vessel morphology. The epidemiologists and other medical/statistical experts can evaluate the association of retinal vessel abnormalities with the biomarkers of systemic diseases. In future, we aim to incorporate the Glaucoma detection module in the aforementioned software system. With the improvement in time efficiency, the proposed methodology can be used as a building block in developing an automated system for early detection of Glaucoma.

References

1. Abramoff, M.D., Garvin, M.K., Sonka, M.: Retinal imaging and image analysis. *IEEE Rev. Biomed. Eng.* **3**, 169–208 (2010)
2. Fraz, M.M., et al.: QUARTZ: quantitative analysis of retinal vessel topology and size – an automated system for quantification of retinal vessels morphology. *Expert Syst. Appl.* **42** (20), 7221–7234 (2015)
3. Illingworth, J., Kittler, J.: The adaptive hough transform. *IEEE Trans. Pattern Anal. Mach. Intell.* **PAMI-9**(5), 690–698 (1987)
4. Luo, X., Liang, T., Wang, W.: Static image segmentation using polar space transformation technique. In: Wong, W.E., Zhu, T. (eds.) *Computer Engineering and Networking*. LNEE, vol. 277, pp. 533–540. Springer, Cham (2014). doi:[10.1007/978-3-319-01766-2_61](https://doi.org/10.1007/978-3-319-01766-2_61)
5. Osareh, A., et al.: Colour morphology and snakes for optic disc localisation. In: *The 6th Medical Image Understanding and Analysis Conference*. BMVA Press (2002)
6. Lee, S., Brady, M.: Optic disk boundary detection. In: Mowforth, P. (ed.) *BMVC91*, pp. 359–362. Springer, London (1991)
7. Lowell, J., et al.: Optic nerve head segmentation. *IEEE Trans. Med. Imaging* **23**(2), 256–264 (2004)
8. Xu, J., et al.: Optic disk feature extraction via modified deformable model technique for glaucoma analysis. *Pattern Recogn.* **40**(7), 2063–2076 (2007)
9. Walter, T., Klein, J.-C.: Segmentation of color fundus images of the human retina: detection of the optic disc and the vascular tree using morphological techniques. In: Crespo, J., Maojo, V., Martin, F. (eds.) *ISMDA 2001*. LNCS, vol. 2199, pp. 282–287. Springer, Heidelberg (2001). doi:[10.1007/3-540-45497-7_43](https://doi.org/10.1007/3-540-45497-7_43)
10. Kande, G.B., Subbaiah, P.V., Savithri, T.S.: Segmentation of exudates and optic disk in retinal images. In: *Sixth Indian Conference on Computer Vision, Graphics and Image Processing, ICVGIP 2008*. IEEE (2008)
11. Stapor, K., Świtonski, A., Chrastek, R., Michelson, G.: Segmentation of fundus eye images using methods of mathematical morphology for glaucoma diagnosis. In: Bubak, M., Albada, G.D., Sloot, P.M.A., Dongarra, J. (eds.) *ICCS 2004*. LNCS, vol. 3039, pp. 41–48. Springer, Heidelberg (2004). doi:[10.1007/978-3-540-25944-2_6](https://doi.org/10.1007/978-3-540-25944-2_6)

12. Lupascu, C.A., Tegolo, D., Di Rosa, L.: Automated detection of optic disc location in retinal images. In: 21st IEEE International Symposium on Computer-Based Medical Systems, CBMS 2008. IEEE (2008)
13. Welfer, D., Scharcanski, J., Marinho, D.R.: A morphologic two-stage approach for automated optic disk detection in color eye fundus images. *Pattern Recogn. Lett.* **34**(5), 476–485 (2013)
14. Basit, A., Fraz, M.M.: Optic disc detection and boundary extraction in retinal images. *Appl. Opt.* **54**(11), 3440–3447 (2015)
15. Aquino, A., Gegúndez-Arias, M.E., Marín, D.: Detecting the optic disc boundary in digital fundus images using morphological, edge detection, and feature extraction techniques. *IEEE Trans. Med. Imaging* **29**(11), 1860–1869 (2010)
16. Morales, S., et al.: Automatic detection of optic disc based on PCA and mathematical morphology. *IEEE Trans. Med. Imaging* **32**(4), 786–796 (2013)
17. Abdullah, M., Fraz, M.M., Barman, S.A.: Localization and segmentation of optic disc in retinal images using circular Hough transform and grow-cut algorithm. *PeerJ* **4**, e2003 (2016)
18. Gonzalez, R.C., Woods, R.E.: *Digital Image Processing*, 3rd edn. Prentice-Hall Inc., Upper Saddle (2006)
19. Hough, P.: Method and means for recognizing complex patterns. Google Patents (1962)
20. Luengo-Oroz, M.A., Faure, E., Angulo, J.: Robust iris segmentation on uncalibrated noisy images using mathematical morphology. *Image Vis. Comput.* **28**(2), 278–284 (2010)
21. Fumero, F., et al.: RIM-ONE: an open retinal image database for optic nerve evaluation. In: 2011 24th International Symposium on Computer-Based Medical Systems (CBMS). IEEE (2011)
22. Odstreilik, J., et al.: Retinal vessel segmentation by improved matched filtering: evaluation on a new high-resolution fundus image database. *IET Image Proc.* **7**(4), 373–383 (2013)
23. Decencière, E., et al.: Feedback on a publicly distributed image database: the Messidor database. *Image Anal. Stereol.* **33**(3), 231–234 (2014)
24. DiaretDb, M.: *DiaRetDB1: Diabetic retinopathy database and evaluation protocol* (2009)
25. Carmona, E.J., et al.: Identification of the optic nerve head with genetic algorithms. *Artif. Intell. Med.* **43**(3), 243–259 (2008)
26. Staal, J., et al.: Ridge-based vessel segmentation in color images of the retina. *IEEE Trans. Med. Imaging* **23**(4), 501–509 (2004)
27. Sopharak, A., et al.: Automatic detection of diabetic retinopathy exudates from non-dilated retinal images using mathematical morphology methods. *Comput. Med. Imaging Graph.* **32**(8), 720–727 (2008)
28. Seo, J., et al.: Measurement of ocular torsion using digital fundus image. In: 26th Annual International Conference of the IEEE Engineering in Medicine and Biology Society, IEMBS 2004. IEEE (2004)
29. Walter, T., et al.: A contribution of image processing to the diagnosis of diabetic retinopathy-detection of exudates in color fundus images of the human retina. *IEEE Trans. Med. Imaging* **21**(10), 1236–1243 (2002)
30. Salazar-Gonzalez, A., et al.: Segmentation of the blood vessels and optic disk in retinal images. *IEEE J. Biomed. Health Inf.* **18**(6), 1874–1886 (2014)